Title

Controlled induction of human pancreatic progenitors produces functional beta-like cells in vitro

Journal

The EMBO Journal, 34(13)

ISSN

0261-4189

Authors

Russ, Holger A
Parent, Audrey V
Ringler, Jennifer J
et al.

Publication Date

2015-07-02

DOI

10.15252/embj.201591058

Peer reviewed

Article

TRANSPARENT PROCESS

THE EMBO JOURNAL

Controlled induction of human pancreatic progenitors produces functional beta-like cells *in vitro*

Holger A Russ[1], Audrey V Parent[1], Jennifer J Ringler[1], Thomas G Hennings[1], Gopika G Nair[1], Mayya Shveygert[2], Tingxia Guo[1,†], Sapna Puri[1], Leena Haataja[3], Vincenzo Cirulli[4], Robert Blelloch[2], Greg L Szot[1], Peter Arvan[3] & Matthias Hebrok[1,*]

Abstract

Directed differentiation of human pluripotent stem cells into functional insulin-producing beta-like cells holds great promise for cell replacement therapy for patients suffering from diabetes. This approach also offers the unique opportunity to study otherwise inaccessible aspects of human beta cell development and function *in vitro*. Here, we show that current pancreatic progenitor differentiation protocols promote precocious endocrine commitment, ultimately resulting in the generation of non-functional polyhormonal cells. Omission of commonly used BMP inhibitors during pancreatic specification prevents precocious endocrine formation while treatment with retinoic acid followed by combined EGF/KGF efficiently generates both PDX1$^+$ and subsequent PDX1$^+$/NKX6.1$^+$ pancreatic progenitor populations, respectively. Precise temporal activation of endocrine differentiation in PDX1$^+$/NKX6.1$^+$ progenitors produces glucose-responsive beta-like cells *in vitro* that exhibit key features of *bona fide* human beta cells, remain functional after short-term transplantation, and reduce blood glucose levels in diabetic mice. Thus, our simplified and scalable system accurately recapitulates key steps of human pancreas development and provides a fast and reproducible supply of functional human beta-like cells.

Keywords beta-like cells; diabetes; human embryonic stem cells; insulin-producing cells, pancreas
Subject Categories Methods & Resources; Molecular Biology of Disease; Stem Cells
DOI 10.15252/embj.201591058 | Received 22 January 2015 | Revised 26 March 2015 | Accepted 1 April 2015 | Published online 23 April 2015
The EMBO Journal (2015) 34: 1759–1772

See also: **FM Spagnoli** (July 2015)

Introduction

Diabetes mellitus type 1 and 2 (T1D, T2D) are diseases characterized by autoimmune destruction or progressive dysfunction and subsequent loss of insulin-producing pancreatic beta cells, respectively. Current treatments for both types of patients with diabetes consist of regulating blood glucose levels through injections of exogenous insulin. While this approach provides reasonable management of the diseases, unwanted risks and long-term complications persist due to the inability of tightly maintaining glucose levels within a normal physiological range. Complications include life-threatening episodes of hypoglycemia, as well as long-term complications from hyperglycemia resulting in micro- and macro-angiopathy leading to cardiovascular pathologies and kidney failure, as well as neuropathy. Thus, there is a need for distinct treatments that provide superior control of glucose metabolism to minimize or ideally eliminate long-term complications.

One existing approach to treating diabetes is transplantation of human cadaveric islet preparations into patients. This procedure typically results in better glycemic control, can render patients insulin independent for prolonged periods of time, and improves overall quality of life (Shapiro *et al*, 2000; Posselt *et al*, 2010; Barton *et al*, 2012). However, the severe shortage of cadaveric organ donors, requirement for lifelong immunosuppression, and variability between islet preparations hampers the use of islet transplantation as a readily available treatment for people with diabetes. Consequently, numerous research efforts have focused on identifying abundant alternative sources of surrogate glucose-responsive insulin-producing cells (Zhou & Melton, 2008; Tudurí & Kieffer, 2011; Efrat & Russ, 2012; Hebrok, 2012; Nostro & Keller, 2012; Bouwens *et al*, 2013; Pagliuca & Melton, 2013). One of the most appealing approaches is the directed differentiation into insulin-producing cells from pluripotent human embryonic stem cells (hESCs)

1 Diabetes Center, University of California San Francisco, San Francisco, CA, USA
2 Eli and Edythe Broad Center of Regeneration Medicine and Stem Cell Research, Center for Reproductive Sciences and Department of Urology, University of California San Francisco, San Francisco, CA, USA
3 Division of Metabolism, Endocrinology & Diabetes, University of Michigan Medical School, Brehm Tower, Ann Arbor, MI, USA
4 Diabetes and Obesity Center of Excellence, Department of Medicine, Institute for Stem Cells and Regenerative Medicine, University of Washington, Seattle, WA, USA
*Corresponding author. Tel: +1 415 514 0820; E-mail: mhebrok@diabetes.ucsf.edu
†Present address: Fluidigm Corporation, South San Francisco, CA, USA

(D'Amour *et al*, 2005; Chen *et al*, 2009; Mfopou *et al*, 2010; Nostro *et al*, 2011; Van Hoof *et al*, 2011; Xu *et al*, 2011; Guo *et al*, 2013b; Shim *et al*, 2014) and, more recently, induced pluripotent stem cells (Maehr *et al*, 2009; Hua *et al*, 2013; Shang *et al*, 2014).

Comprehensive knowledge of signaling events and temporal transcription factor (TF) expression patterns during rodent pancreas organogenesis (Hebrok, 2003; Murtaugh & Melton, 2003; Pan & Wright, 2011; Seymour & Sander, 2011) have accelerated the identification of culture conditions that allow the generation of pancreatic cell types from human pluripotent stem cells (hPSCs). Early developmental stages, including definitive endoderm, gut tube-like cells, and pancreatic progenitors can be efficiently induced *in vitro*. However, subsequent transitions toward hormone-expressing cells *in vitro* are less efficient and frequently lead to the formation of a mixed population of different pancreatic progenitors and polyhormonal endocrine cells (D'Amour *et al*, 2006; Nostro *et al*, 2011; Guo *et al*, 2013a). Such polyhormonal cells express insulin among other hormones, but lack expression of key beta cell transcription factors and do not secrete insulin *in vitro* in response to a glucose challenge—the hallmark function of *bona fide* beta cells (D'Amour *et al*, 2006; Nostro *et al*, 2011; Guo *et al*, 2013a). Nonetheless, transplantation of such heterogeneous cultures into surrogate mice results in the formation of glucose-responsive beta-like cells after several months *in vivo* (Kroon *et al*, 2008; Rezania *et al*, 2012; Szot *et al*, 2015). Sophisticated sorting experiments identified progenitor cells expressing pancreatic and duodenal homeobox 1 TF (PDX1, also known as IPF1) and homeobox protein NKX6.1 as the source for these functional beta-like cells (Kelly *et al*, 2011). While polyhormonal cells have been identified in human fetal pancreas, suggesting that they may reflect aspects of the normal embryonic differentiation process (De Krijger *et al*, 1992; Riedel *et al*, 2011), increasing evidence indicates that hESC-derived polyhormonal cells preferentially give rise to single-hormone-positive alpha-like cells (Rezania *et al*, 2011). Thus, to fully replicate human beta cell development *in vitro,* it is imperative to better understand and accurately recapitulate the sequence of embryonic signals required for the proper specification of beta cell precursors, rather than alpha cell precursors.

During normal *in vivo* pancreatic organogenesis, functional beta cells are generated through a stepwise specification process starting with pancreatic progenitors, identified by the expression of Pdx1 (Herrera *et al*, 2002). While $Pdx1^+$ cells can give rise to all pancreatic lineages (Herrera *et al*, 2002), the subsequent induction of Nkx6.1 in these cells restricts their differentiation potential to only endocrine and ductal cells (Schaffer *et al*, 2010). Endocrine differentiation is then initiated in $Pdx1^+/Nkx6.1^+$ progenitors by short-lived expression of the basic helix loop helix TF neurogenin 3 (Neurog3, also known as Ngn3) (Gu *et al*, 2002). Interestingly, the timing of Neurog3 expression has been shown to be crucial in promoting the formation of diverse endocrine islet cell types (Johansson *et al*, 2007). For example, precocious induction of endocrine differentiation by forced expression of Neurog3 in mice results predominantly in the generation of alpha cells (Johansson *et al*, 2007). Given that hESC-derived polyhormonal cells have been shown to give rise to alpha cells (Rezania *et al*, 2011), we hypothesized that the *in vitro* generation of polyhormonal endocrine cells results from premature assignment to the endocrine fate.

To address this issue, we performed a detailed stepwise analysis of pancreatic progenitor generation and endocrine induction. Most current protocols efficiently establish $PDX1^+$ progenitors by using retinoic acid in combination with molecules to inhibit bone morphogenic protein (BMP) and sonic hedgehog (SHH) signaling pathways, while simultaneously adding either fibroblast growth factor 10 or keratinocyte growth factor (KGF, also known as FGF7) (Mfopou *et al*, 2010; Nostro & Keller, 2012; Rezania *et al*, 2012; Guo *et al*, 2013b; Hua *et al*, 2013). Here, we show that the use of BMP inhibitors to specify pancreatic cells promotes the precocious induction of endocrine differentiation in $PDX1^+$ pancreatic progenitors, which results in the formation of polyhormonal cells. Furthermore, we have identified simplified culture conditions that replicate fetal endocrine development and allow for the precise and efficient generation of $PDX1^+$ and $PDX1^+/NKX6.1^+$ progenitor populations without precocious activation of the endocrine marker NEUROG3. Importantly, subsequent induction of endocrine differentiation in correctly specified $PDX1^+/NKX6.1^+$ progenitor cells results in the formation of glucose-responsive insulin-expressing beta-like cells *in vitro* within less than 3 weeks. Our study therefore details a simplified directed differentiation protocol that closely recapitulates key aspects of human endocrine development and results in the formation of large numbers of glucose-responsive beta-like cells under cell culture conditions.

Results

Pancreatic differentiation of hESCs using a large-scale culture system results in two distinct subsets of insulin-producing cells

To generate pancreatic beta-like cells from human PSC, we established a scalable three-dimensional suspension culture system based on previously reported methods (Rezania *et al*, 2012; Schulz *et al*, 2012) (Fig 1A). To monitor the generation of live insulin-producing cells and facilitate their isolation, we employed the recently published $INS^{GFP/W}$ reporter cell line (Micallef *et al*, 2012) in which green fluorescence protein (GFP) expression is under the control of the endogenous insulin promoter. Using this differentiation protocol, GFP reporter expression was readily observed at day 13 and increased thereafter, resulting in an average of $37 \pm 8\%$ GFP^+ cells between days 19 and 24 (Fig 1B–D). The validity of GFP as an accurate substitute for insulin was verified by staining with an insulin specific antibody, which revealed an even higher percentage of insulin-producing cells (up to 60%) likely due to delayed accumulation of the fluorescence marker (Fig 1E). Similar results were obtained with an antibody specific to human C-peptide, excluding antibody reactivity due to insulin uptake from culture media (Fig 1E). Co-staining for human C-peptide and glucagon (GCG), a hormone normally produced by alpha cells, showed that 4.3% and 13.2% of all cells exhibited a polyhormonal phenotype at day 13 and day 19, respectively (Fig 1F). Co-staining for C-peptide and NKX6.1 at day 20 indicated the presence of some double-positive beta-like cells (Fig 1G). Quantitative flow cytometry analysis revealed that the proportion of insulin and NKX6.1 double-positive beta-like cells increased from less than 2.5% at day 13 to approximately 12% cells at day 19 of total cells (Fig 1G). Ultrastructural analysis of differentiated cultures showed cells containing secretory vesicles with an

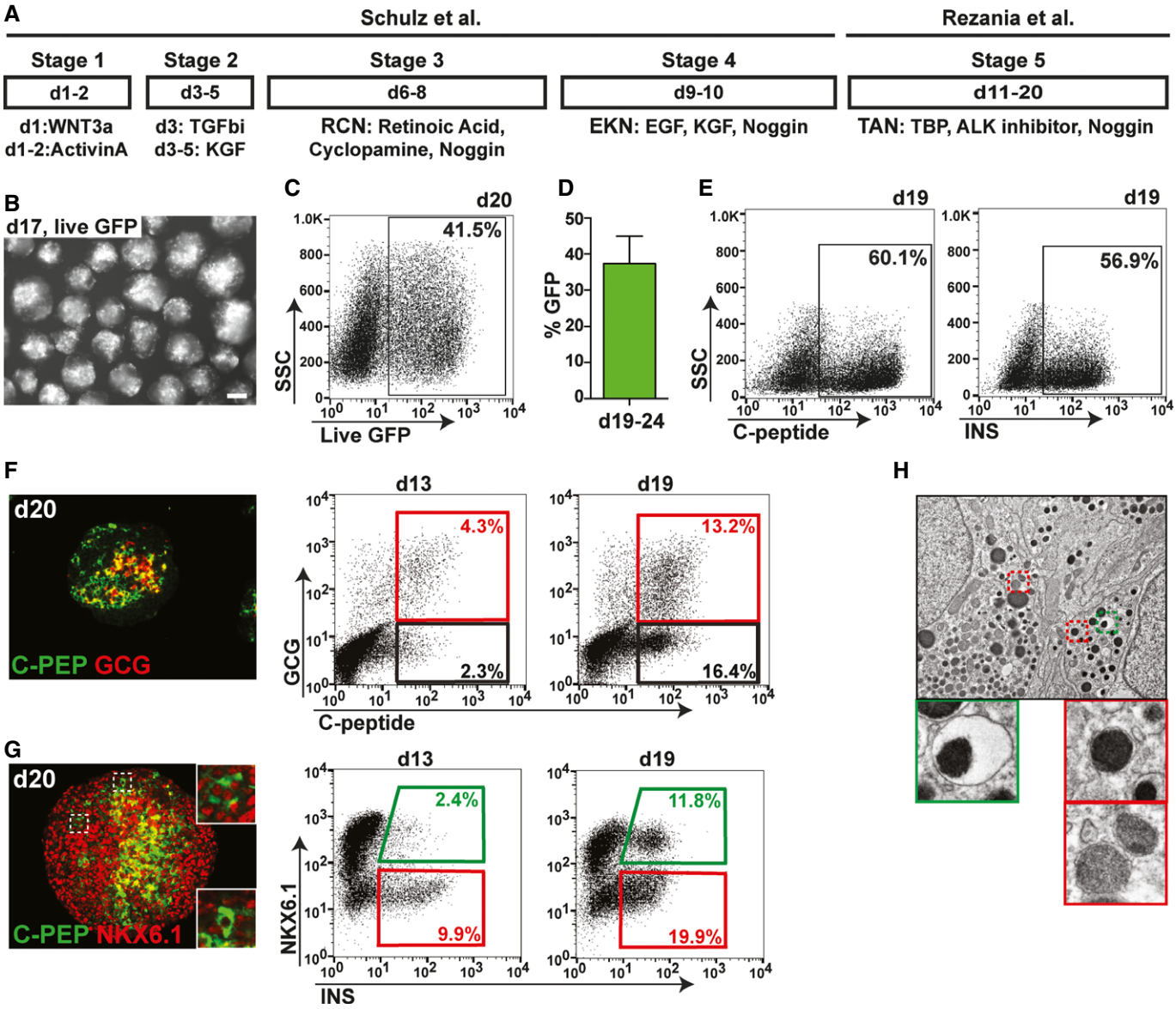

Figure 1. Pancreatic differentiation of hESCs using a large-scale culture system results in two distinct subsets of insulin-producing cells.

A Schematic outlining the differentiation protocol employed. R, retinoic acid; C, cyclopamine; N, Noggin, E, epidermal growth factor; K, keratinocyte growth factor; T, TBP; A, ALK inhibitor.

B Micrograph of MEL1$^{INS-GFP}$ cell clusters after 17 days of differentiation demonstrating strong GFP expression (GFP expression in white). Scale bar, 200 μm.

C Flow cytometric analysis at day 20 of differentiation showing 41.5% of all cells expressing GFP under the control of the endogenous insulin promoter.

D Quantification by flow cytometry of the average percentage of GFP$^+$ cells within differentiated cultures after 19–24 days. n = 7. Values are average ± standard deviation (SD).

E Flow cytometric analysis of intracellular human-specific C-peptide (C-PEP) and insulin (INS) shows comparable percentages of C-PEP$^-$ and INS$^+$ cells.

F Immunofluorescence staining for C-PEP and glucagon (GCG), and flow cytometric quantification of GCG$^+$/C-PEP$^+$ (red gate) and GCG$^-$/C-PEP$^+$ (black gate) populations at days 13 and 19 of differentiation.

G Immunofluorescence staining for C-PEP and NKX6.1, and flow cytometric quantification of NKX6.1$^+$/INS$^+$ (green gate) and NKX6.1$^-$/INS$^+$ (red gate) populations at day 13 and 19. Immunofluorescence insets show two distinct phenotypes for C-PEP$^+$ cells (NKX6.1$^+$ and NKX6.1$^-$). A robust INS/NKX6.1 double-positive population is only detected at day 19.

H Transmission electron microscopy of day 20 clusters. Cells contain both secretory vesicles with electron-dense cores surrounded by electron-light halos (green box), akin to *bona fide* beta cell vesicles, as well as other granules similar to those found in non-beta pancreatic cells (red boxes).

electron-dense core surrounded by an electron-light halo (Fig 1H), a morphology reminiscent of insulin vesicles that are found in human beta cells. However, the majority of cells exhibited a mixture of secretory granules usually found in non-beta cells of human pancreas preparations (Fig 1H). Thus, differentiation experiments employing published protocols (Rezania *et al*, 2012; Schulz *et al*,

2012) result in the efficient generation of two distinct insulin-producing cell populations: INS^+ cells that do not co-express the critical TF NKX6.1 and manifest as polyhormonal cells, and $INS^+/NKX6.1^+$ beta-like cells that more closely resemble human beta cells. Notably, $INS^+/NKX6.1^+$ beta-like cells are absent from cultures at earlier time points but appear and increase in number at later stages of differentiation, suggesting that they are derived from a distinct progenitor cell type.

Defining the temporal activities of individual signaling factors to efficiently generate $PDX1^+$ and $PDX1^+/NKX6.1^+$ pancreas progenitor populations while preventing precocious induction of endocrine differentiation

To characterize the type of progenitors present in differentiating cultures at the point of endocrine induction, we performed a detailed time-course analysis for the expression of pancreatic markers PDX1, NKX6.1, NEUROG3, GCG, and INS (Supplementary Fig S1). High expression of the progenitor marker PDX1 was efficiently induced and maintained starting 1 day after the combined addition of retinoic acid (R), the SHH inhibitor cyclopamine (C), and the BMP inhibitor Noggin (N) to the culture media (referred to as RCN, day 6, Supplementary Fig S1A and B). Subsequent treatment with epidermal growth factor (EGF), KGF, and N (EKN) resulted in the robust generation of $PDX1^+/NKX6.1^+$ double-positive cells, reaching 67% of the total population at day 11 (Supplementary Fig S1A and B). Immunofluorescence analysis revealed that the RCN cocktail of factors widely used to generate pancreatic endoderm also induces precocious expression of NEUROG3 in $PDX1^+$ pancreatic progenitors. Indeed, the expression of NEUROG3 can be detected as early as day 6, when NKX6.1 protein is absent from all cells (Supplementary Fig S1A and B). Consequentially, insulin-expressing cells that are first detected 4 days after NEUROG3 induction (starting at day 10) do not co-express NKX6.1 and are mostly polyhormonal (Fig 1F and G, and Supplementary Fig S1C). In contrast, INS/NKX6.1 double-positive beta-like cells can be readily detected only at later time points (day 19, Fig 1G), suggesting that these cells differentiate from PDX1/NKX6.1 double-positive progenitor cells. We thus hypothesized that robust generation of $PDX1^+/NKX6.1^+$ progenitor cells prior to induction of NEUROG3 would allow efficient generation of beta-like cells *in vitro*. To determine which of the factors used between days 6 and 8 in the original protocol (R, C, and N) are responsible for the induction of PDX1, NKX6.1, and NEUROG3, we incubated spheres with each of the factors alone or in different combinations over days 6–8 (Fig 2A). Basal media with B27 but lacking any additional factors served as the control condition. At the end of day 8, each of these six conditions was further subdivided into three different treatment groups: Media composition remained the same as during days 6–8 (group 1) or changed either to EK (group 2) or to EKN (group 3), resulting in 18 individual experimental conditions (Fig 2A). Spheres cultured under each condition were analyzed at day 9.5 by flow cytometry to quantify the expression of PDX1 and NKX6.1, and by conventional immunofluorescence analysis for NKX6.1 and NEUROG3 expression. As shown in Fig 2B, spheres within group 1 that had been exposed to retinoic acid during days 6–8, either alone or in combination with other factors (conditions 4, 5, and 6), exhibited highly efficient generation of $PDX1^+$ progenitors (> 88%), while the addition of C or N alone (conditions 2 and 3) did not result in enhanced generation of $PDX1^+$ cells over basal media alone. NKX6.1 was induced only weakly in all group 1 conditions, with the exception of RC (condition 5), which produced 45% PDX1/NKX6.1 double-positive cells. NKX6.1 expression was also strongly induced when cells were exposed to retinoic acid alone or in combination with other factors followed by treatment with EK (group 2) or EKN (group 3) (Fig 2B and C, conditions 10–12 and 16–18). Endocrine differentiation, marked by NEUROG3 expression, was noted only when spheres had been exposed to N, either between days 5 and 9.5 (Fig 2C, conditions 3, 6, 9, and 12) or starting at the end of day 8 (Fig 2C, group 3, conditions 13–18). Very few $NEUROG3^+$ cells were detected in all other conditions (Fig 2C, conditions 1, 2, 4, 5, 7, 8, 10, and 11). qPCR analysis at day 8 of NEUROG3 and its downstream target NKX2.2 mRNA transcripts revealed significantly lower levels of these endocrine markers with R treatment when compared to the commonly employed RCN condition (Supplementary Fig S1D). Notably, the addition of vitamin C, recently shown to reduce endocrine differentiation in hESCs (Rezania *et al*, 2014), did not significantly lower NEUROG3 or NKX2.2 transcripts in our suspension culture system during RCN or R treatment (Supplementary Fig S1D). Taken together, these results indicate that R followed by EK treatment leads to highly efficient generation of $PDX1^+/NKX6.1^+$ progenitors (90%) and that the formation of *bona fide* NEUROG3-positive endocrine precursors is induced by treatment with N (Fig 2A–C, condition 10, green gates). Thus, by defining the temporal activities of individual signaling factors alone and in combination, we can induce transcription factor expression patterns characteristic of different human embryonic pancreatic progenitor cells types ($PDX1^+$ and $PDX1^+/NKX6.1^+$ progenitors) without precocious induction of endocrine differentiation.

Recapitulating human pancreas organogenesis to generate endocrine progenitors

This improved and simplified differentiation protocol provides the basis for subsequent efficient formation of insulin-producing cells in suspension (Fig 3A). Endocrine differentiation in PDX1/NKX6.1 double-positive cells was induced by exposure to a cocktail of factors consisting of TBP (T), ALK inhibitor (A), N, and K, (TANK) which have previously been shown to activate NEUROG3 expression while maintaining high expression of PDX1 and NKX6.1 (Nostro *et al*, 2011; Rezania *et al*, 2012) (Fig 3A and B). Importantly, while NEUROG3 protein was undetectable before TANK treatment (Fig 3C, day 9), cells exhibiting nuclear accumulation of NEUROG3 protein appeared as early as 1 day following TANK treatment (Fig 3C, day 10). Thus, the expression of the pro-endocrine factor NEUROG3 is rapidly induced through TANK treatment once $PDX1^+/NKX6.1^+$ progenitors are specified (Fig 3B, day 9). In contrast to the near-uniform generation of $PDX1^+$ and $PDX1^+/NKX6.1^+$ progenitor populations following appropriate stimulation, endocrine differentiation appears to be confined to a smaller population of cells. This observation can be explained by the very short half-life of the NEUROG3 protein (Roark *et al*, 2012), which allows only transient detection of this marker in cells undergoing endocrine differentiation. However, $NEUROG3^+$ cells continued to be present when clusters were exposed to the endocrine differentiation cocktail for 5 days (Fig 3C, day 14), indicating that endocrine cells were being

A

Condition	Factors d6-8	d9-9.5	
1	Base	Base	Group 1
2	C	C	
3	N	N	
4	R	R	
5	RC	RC	
6	RCN	RCN	
7	Base	EK	Group 2
8	C	EK	
9	N	EK	
10	R	EK	
11	RC	EK	
12	RCN	EK	
13	Base	EKN	Group 3
14	C	EKN	
15	N	EKN	
16	R	EKN	
17	RC	EKN	
18	RCN	EKN	

BASE=B27 only control, R= Retinoic acid, C= Cyclopamine, N= Noggin, E=EGF, K= KGF.

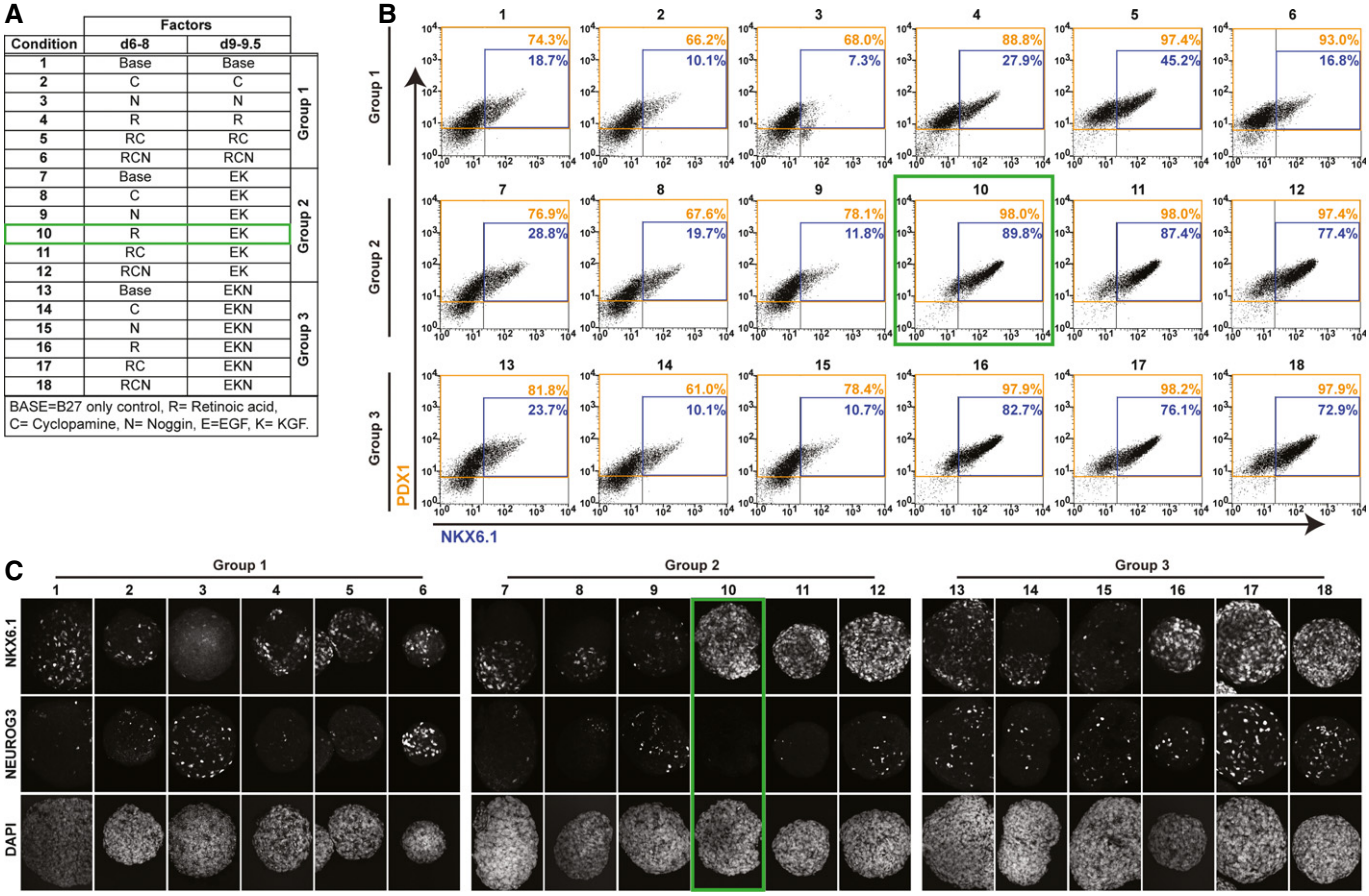

Figure 2. Defining the temporal activities of individual signaling factors to efficiently generate PDX1$^+$ and PDX1$^+$/NKX6.1$^+$ pancreatic progenitor populations while preventing precocious induction of endocrine differentiation.

A–C Pancreatic progenitor marker expression at day 9.5 after treatment with conventional differentiation factors alone or in different combinations. Treatments consisted of combinations of cyclopamine (C), Noggin (N), and retinoic acid (R) during days 6–8 followed by subdivision of each condition into three treatment groups during day 9–9.5. Group 1: continuation of day 6–8 treatment; Group 2: treatment with EGF and KGF (EK); Group 3: treatment with EGF, KGF, and Noggin (EKN). The condition selected for further studies (10) is marked with a green box. Data shown are representatives of results obtained in two independent experiments. (A) Table detailing 18 different culture conditions that were evaluated. (B) Quantification of PDX1 (orange gate) and NKX6.1 (blue gate) protein-expressing cells in individual conditions after 9.5 days of differentiation. (C) NKX6.1 and NEUROG3 protein expression assessed by whole-mount staining of differentiated clusters at 9.5 days. Note robust NEUROG3 expression in all clusters exposed to N (conditions 3, 6, 9, and 12–18).

generated throughout this period. To further characterize the progenitors present in our cultures at the initiation of endocrine differentiation, we analyzed the expression of NKX2.2, a downstream target of NEUROG3. NKX2.2 has recently been reported to have distinct expression patterns during pancreatic organogenesis in mouse and human (Jennings *et al*, 2013). While Nkx2.2 is readily detectable in mouse pancreatic progenitor cells before Neurog3 expression, NKX2.2 protein is only observed after endocrine commitment during human pancreas development. Similarly, we detected NKX2.2 protein expression only after endocrine differentiation is initiated at day 10, but not before in either PDX1$^+$ or PDX1$^+$/NKX6.1$^+$ progenitors (Fig 3C, data not shown). Of note, some NKX2.2$^+$ cells at day 10 co-express NEUROG3, and increasing numbers of NKX2.2$^+$/NEUROG3$^-$ cells are found at later time points (Fig 3C). These data suggest that NKX2.2 could serve as a lineage tracer for human cells that have undergone endocrine differentiation induced by transient NEUROG3 expression. In summary, we have established a novel differentiation strategy that faithfully recapitulates human pancreas organogenesis and allows for the precise control over the generation of PDX1$^+$ and PDX1$^+$/NKX6.1$^+$ progenitors.

Efficient generation of PDX1$^+$/NKX6.1$^+$ pancreatic progenitor cells prior to endocrine induction results in glucose-responsive beta-like cells

To test the hypothesis that precocious activation of NEUROG3 expression results in immature polyhormonal cells and not INS/NKX6.1 double-positive beta-like cells, we initiated endocrine differentiation at day 7 in PDX1$^+$ pancreatic progenitors by exposing the cells to NEUROG3 inducers ALKi and Noggin (Supplementary Fig S2A). While some single-hormone-positive cells were present at day 13, many endocrine cells were double-positive for C-peptide and glucagon (Supplementary Fig S2B). In further support of our hypothesis, virtually all C-peptide-positive cells lacked expression of

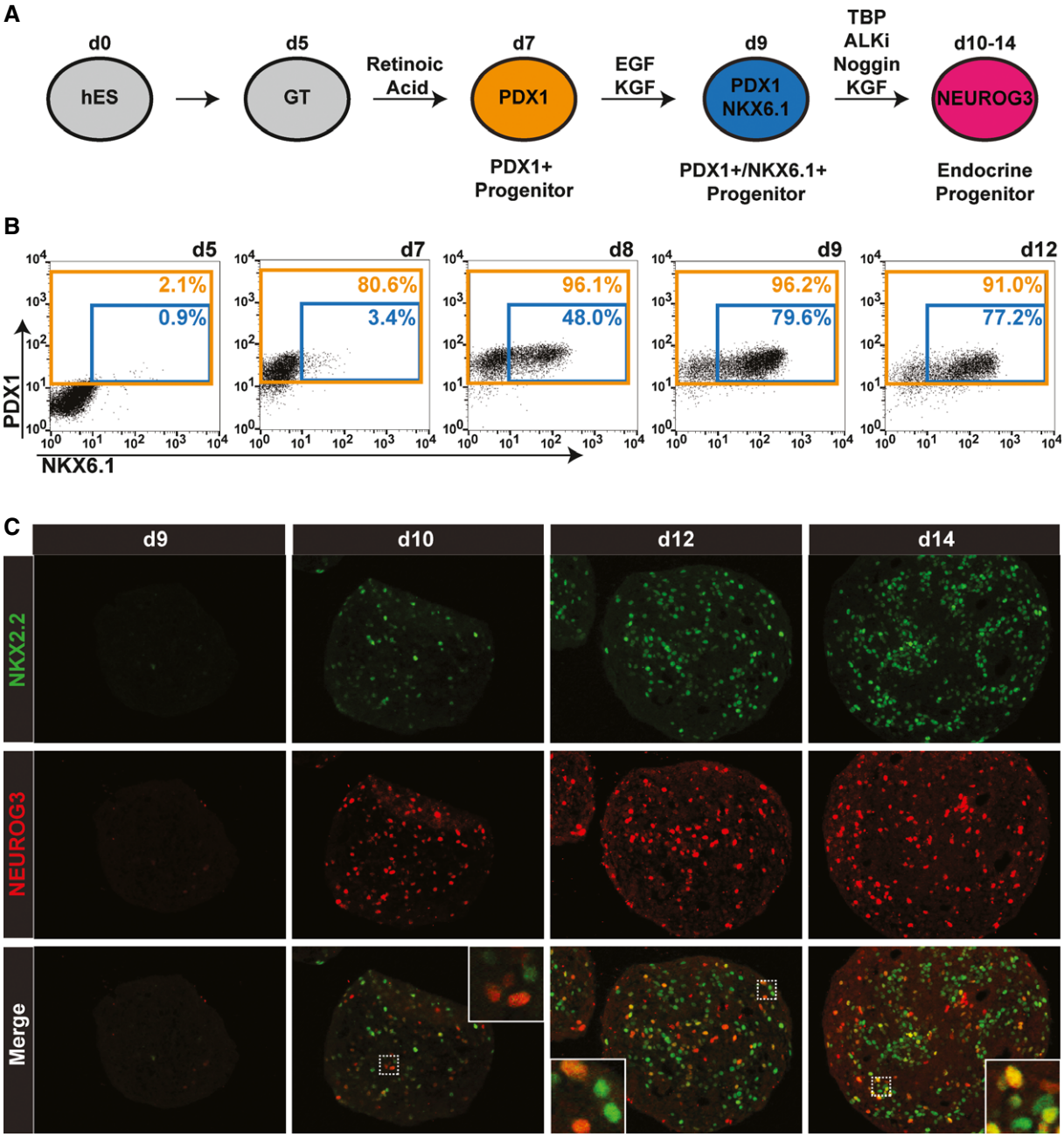

Figure 3. Recapitulating human pancreas organogenesis to generate endocrine progenitors.

A Schematic outlining a simplified differentiation strategy for the controlled, stepwise generation of pancreatic progenitor cell types.

B Time-course flow cytometric analysis illustrates the efficient generation of PDX1$^+$ progenitor (orange gate) and PDX1$^+$/NKX6.1$^+$ progenitor (blue gate) populations. Data from one of three independent experiments with similar results are shown.

C Immunofluorescence analysis of sections from differentiated clusters at indicated time points stained for human NKX2.2 (green) and NEUROG3 (red). Insets show NEUROG3/NKX2.2 double-positive cells. Data from one of three independent experiments with similar results are shown.

NKX6.1 (Supplementary Fig S2C). To test whether correctly specified PDX1$^+$/NKX6.1$^+$ progenitor cells undergo differentiation toward INS/NKX6.1 double-positive beta-like cells, we transferred spheres differentiated using our new method into a basal media without additional growth factors and monitored the establishment of beta-like cells (Fig 4A). The percentage of GFP$^+$ cells increased from day 13 to day 19, reaching an average of 23 ± 6% human C-peptide-positive cells at days 19–21, likely reflecting continuous generation of insulin-producing cells for ~4 days after removal of NEUROG3-inducing factors (Fig 4B and C). Immunofluorescence analysis of insulin-producing cells revealed co-expression and nuclear localization of TFs critical for beta cell function (PDX1,

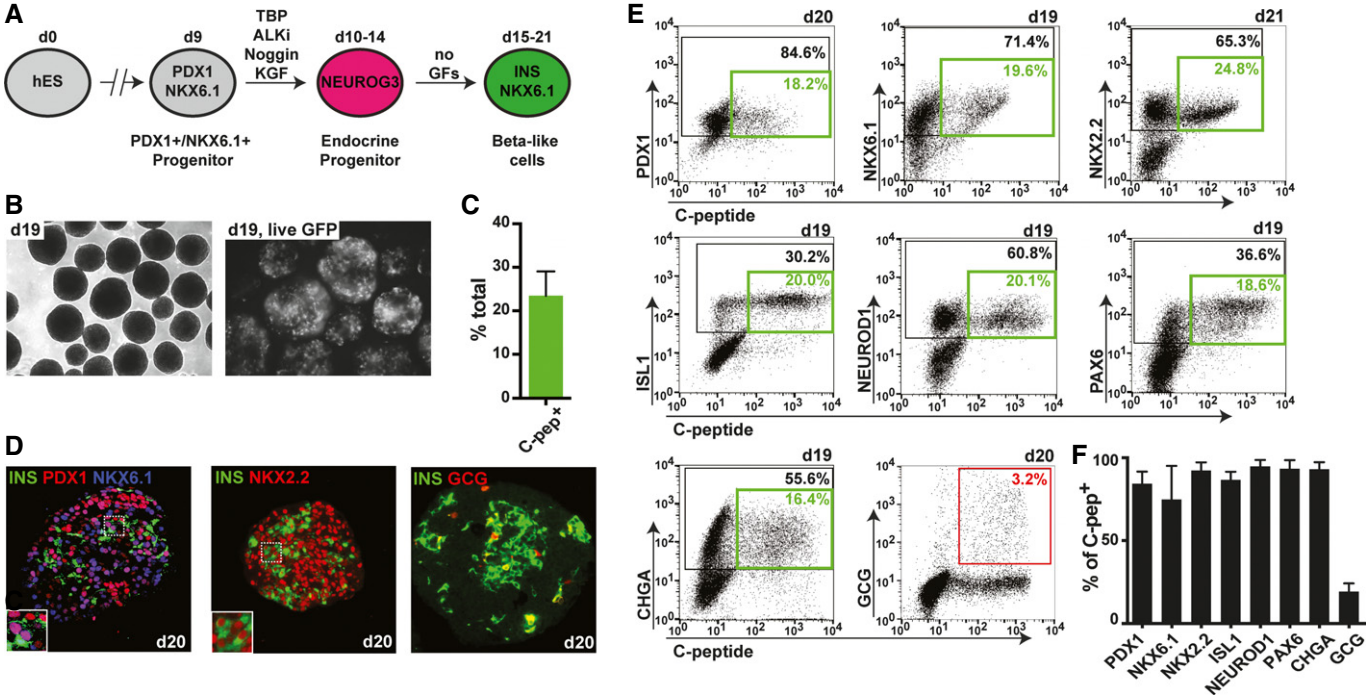

Figure 4. Efficient generation of PDX1$^+$/NKX6.1$^+$ pancreatic progenitor cells prior to endocrine induction results in beta-like cells.

A Schematic outlining a simplified differentiation strategy for the controlled, stepwise generation of pancreatic progenitor and subsequent endocrine cell types. GFs, growth factors.

B Micrographs of differentiated clusters at day 19 under light microscopy (left picture) or fluorescent microscopy showing prominent GFP expression (right picture; GFP expression shown in white).

C Quantification of the percentage of human C-peptide-positive cells at day 19–21. Values are average ± SD. *n* = 7 independent experiments.

D Immunofluorescence stainings of differentiated clusters at day 20 for insulin (INS), PDX1, NKX6.1, NKX2.2, and glucagon (GCG). One of four experiments with similar outcome is shown.

E Representative flow cytometry plots depicting co-expression of pancreatic markers PDX1, NKX6.1, NKX2.2, ISL1, NEUROD1, PAX6, chromogranin A (CHGA), and GCG with human C-peptide at indicated time points. Black gates mark percentage of total cells positive for indicated marker on *y*-axis. Green gates mark percentage of double-positive beta-like cells. The red gate marks percentage of INS$^+$/GCG$^+$ bihormonal cells.

F Flow cytometric quantification of C-peptide-positive beta-like cells co-expressing markers in (E). A high percentage of beta-like cells co-express all genes usually found in beta cells, but not the hormone GCG. Values are average ± SD. *n* = 4 for PDX1, *n* = 19 for NKX6.1, *n* = 4 for NKX2.2, *n* = 9 for ISL1, *n* = 9 for NEUROD1, *n* = 5 for PAX6, *n* = 6 for CHGA, and *n* = 5 for GCG. Analysis was performed at days 15–21 of differentiation.

NKX6.1, and NKX2.2), but very few polyhormonal cells (Fig 4D). Flow cytometry analysis of differentiated clusters showed a high percentage of total cells (black gates) and C-peptide-positive beta-like cells (green gates) co-staining for PDX1, NKX6.1, NXK2.2, ISL1, PAX6, NEUROD1, and chromogranin A (CHGA) (Fig 4E). These markers are normally found in both pancreatic progenitors and mature beta cells. Quantification of C-peptide$^+$ beta-like cells co-staining for PDX1, NKX6.1, NKX2.2, ISL1, NEUROD1, PAX6, and CHGA showed 84 ± 7%, 75 ± 20%, 92 ± 5%, 86 ± 5%, 95 ± 4%, 93 ± 5%, and 93 ± 4% double-positive cells, respectively (Fig 4F). Notably, only 3.2% of all differentiated cells co-expressed C-peptide and the hormone glucagon (Fig 4E, red gate). An important hallmark of mature human beta cells is their restricted proliferative capacity. While 9.1 ± 3.7% of C-peptide-negative cells were actively proliferating, only 0.5 ± 0.6% of C-peptide$^+$ beta-like cells co-stain for the proliferation marker Ki-67, indicating their terminal differentiation state (Supplementary Fig S3A and B). Thus, our optimized differentiation strategy results in the predominant generation of post-mitotic, insulin-producing beta-like cells that co-express critical beta cell markers.

To further characterize gene expression in beta-like cells at days 19–20, we took advantage of the GFP live marker to compare sorted GFP$^+$ beta-like cells and GFP$^-$ populations to purified human islets. hESC-derived beta-like cells showed high levels of insulin gene transcripts, comparable to cadaveric islet preparations, while GFP-negative populations exhibit only insignificant levels of the hormone (Fig 5A). We also detected transcript levels for two other hormones (GCG and SST) in GFP$^+$ cells, likely due to contamination by the small number of polyhormonal cells also expressing the GFP reporter (Figs 5A and 4D and E). Consistent with the immunofluorescence analysis (Fig 4D), transcripts for the TFs PDX1, NKX6.1, and NKX2.2 normally found in both progenitor and mature beta cells were expressed at comparable levels in GFP$^-$, GFP$^+$, and islet cells (Fig 5B). Transcripts for the mature human beta cell transcription factors MAFA and MAFB were robustly expressed in human islets and enriched in beta-like cells compared to GFP$^-$ populations. MAFB transcript levels in beta-like cells were similar to human islets; MAFA expression levels were slightly lower (Fig 5B). Other genes important for human beta cell functionality, including the K^{ATP} channel components potassium inwardly rectifying

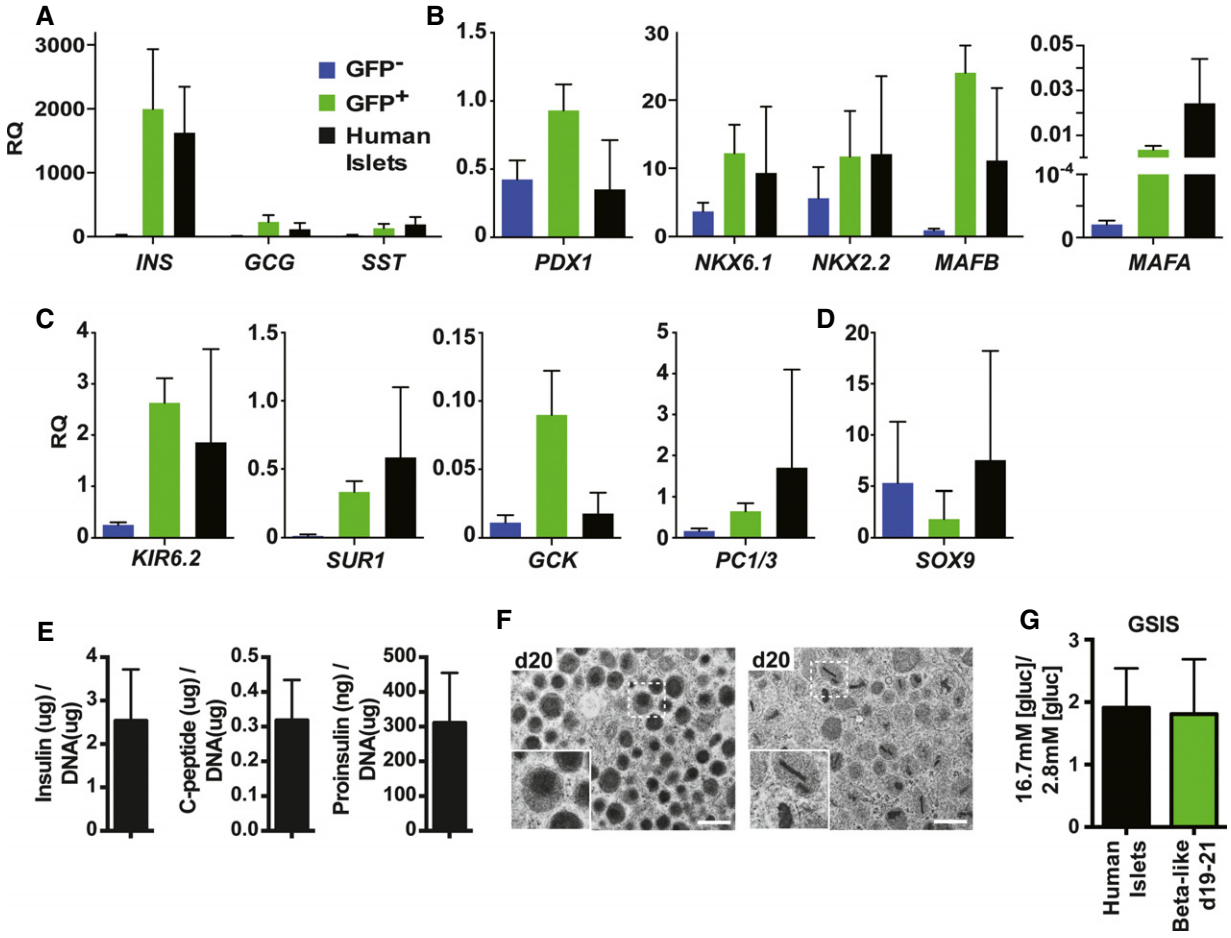

Figure 5. Beta-like cells exhibit key features of *bona fide* human beta cells and are glucose responsive.

A–D Quantitative PCR analysis of selected gene transcripts in sorted GFP$^+$ beta-like cells (green bars), GFP$^-$ populations (blue bars) and human islet preparations (black bars). Results shown relative to the endogenous control GAPDH. RQ, relative quantification. Values are average ± SD. n = 4 independent experiments for hESC-derived cell populations at days 19–20 and n = 3 for human islets.

E Insulin, human C-peptide, and proinsulin content relative to DNA in beta-like cells at day 19. Data presented are average ± standard error (n = three independent experiments, technical duplicates).

F Transmission electron microscopy images of beta-like cells at day 20. One of three experiments with similar results is shown. Scale bar, 500 nm. Insets represent secretory vesicles akin to granules present in *bona fide* human beta cells.

G Glucose-stimulated insulin secretion (GSIS) of human islets and beta-like cells at days 19–20. *Y*-axis indicates ratio of insulin secreted in low glucose conditions to that secreted in high glucose conditions. Values are average ± standard deviation (SD). n = 3 for human islets and n = 10 for beta-like cells.

channel, subfamily J, member 11 (KIR6.2, also known as KCJN11) and ATP-binding cassette, subfamily C, member 8 (SUR1, also known as ABCC8), the glucose metabolism enzyme glucokinase (GCK, also known as HK4), and the prohormone convertase 1/3 (PC1/3) necessary for insulin biosynthesis, were enriched in GFP-positive beta-like cells at levels similar to or exceeding those found in human islets (Fig 5C). In contrast, mRNA levels for the progenitor marker SOX9 were reduced in beta-like cells compared to GFP$^-$ progenitors (Fig 5D). The somewhat higher SOX9 expression in human islets is likely the result of contamination with SOX9-positive duct cells. Thus, our gene expression analysis suggested that hESC-derived beta-like cells possess the molecular machinery necessary for beta cell function, including insulin biosynthesis and glucose metabolism. Further investigations revealed that day 19 beta-like cells contain 2.5 ± 1.2 μg, 0.32 ± 0.12 μg, and 310 ± 143 ng insulin, human C-peptide, and proinsulin per μg DNA, respectively (Fig 5E). These values are comparable to ~2.8 μg insulin, ~0.55 μg C-peptide, and ~150 ng proinsulin per μg DNA for human islets as recently published (Rezania *et al*, 2014). Western blot analysis for proinsulin and mature insulin further confirmed efficient insulin protein processing in hESC-derived beta-like cells, reaching 59 ± 2% of the extent of processing observed in purified human islets (Supplementary Fig S4A and B). Ultrastructural analysis of differentiated cell clusters by transmission electron microscopy revealed that many cells contained secretory vesicles exhibiting electron-dense cores or rod-like structures, akin to what is observed in human beta cells (Fig 5F). To further investigate the functional properties of *in vitro* differentiated beta-like cells, we performed glucose-stimulated insulin secretion assays, in which we measured the release of human C-peptide, a by-product of endogenous insulin

biosynthesis secreted in an equimolar ratio to insulin. hESC-derived beta-like cells analyzed at days 19–21 responded to an increase in glucose concentration from 2.8 mM to 16.7 mM by secreting 1.8 ± 0.9 fold more C-peptide, a response similar to the 1.9 ± 0.6-fold increase detected with human islets (Fig 5G). Thus, beta-like cells generated by our optimized differentiation strategy express critical beta cell genes, synthesize high levels of mature insulin, exhibit ultrastructural features of *bona fide* beta cells, and secrete endogenous insulin in response to changes in physiological concentrations of glucose.

hESC-derived beta-like cells remain glucose responsive after short-term transplantation

To determine whether hESC-derived beta-like cells can maintain their glucose responsiveness *in vivo*, we transplanted approximately 5 million cells under the kidney capsule of immunodeficient mice (days 19–21 spheres consisting of progenitors and beta-like cells). Mice transplanted with 4,000 human islets served as controls. Seven to 10 days post-surgery, human C-peptide levels were measured in overnight fasted mice, before and after the administration of a glucose bolus. As expected, mice that received human islet grafts exhibited low levels of insulin secretion upon fasting, followed by a marked increase in circulating insulin after glucose challenge (average of 221 ± 116 pM, Fig 6A). Similar to mice carrying human islets, fasted mice transplanted with hESC-derived beta-like cells had low levels of circulating C-peptide. Upon glucose administration, C-peptide concentrations in sera of these mice also increased, albeit at lower levels than in mice transplanted with human islets (average of 40 ± 28 pM, Fig 6A). This lower number might be explained in part by the different numbers of cells transplanted in the human islet and beta-like cell groups. Indeed, each human islet contains on average 1,000 cells, of which 50% are beta cells (Cabrera *et al*, 2006). Thus, 4,000 human islets contain approximately 2.0×10^6 *bona fide* beta cells. Since hESC-differentiated spheres contain on average 23% beta-like cells, only about 1.15×10^6 beta-like cells were transplanted per mouse. Normalization based on beta cell number indicates that hESC-derived beta-like cells secreted 70 ± 48 pM human C-peptide per 2.0×10^6 cells, representing approximately one-third of the insulin secreted from each human cadaveric beta cell (Fig 6A). Hematoxylin and eosin staining, together with immunofluorescence analysis of the hESC grafts at 2 weeks post-transplantation, demonstrated prominent islet-like structures positive for human C-peptide (Fig 6B and C). Beta-like cells also maintained co-expression of the key beta cell TFs PDX1, NKX6.1, and NKX2.2, and only few cells co-expressed other hormones such as glucagon and somatostatin (Fig 6C). To further investigate the functional properties of hESC-derived beta-like cells *in vivo*, we transplanted clusters under the kidney capsule of mice rendered diabetic through treatment with the beta cell toxin streptozotocin. Mice that received grafts exhibit significantly reduced blood glucose (BG) levels at all time points analyzed when compared to control animals (Fig 6D). While BG levels were significantly reduced in graft-bearing mice, they continued to exhibit hyperglycemic BG values over time. This is likely due to the limited number of beta-like cells that can be transplanted under the kidney capsule in one mouse. It has previously been shown that 4,000 human islets are required to establish long-term euglycemia in diabetic mice. Transplantation of a smaller number of human islets (1,500 islets) reduces blood glucose levels only for 7 days post-transplantation, after which hyperglycemia returned (Fiaschi-Taesch *et al*, 2010). Our surgical procedure permits the transplantation of ~1.15×10^6 beta-like cells, substantially less than the ~2.0×10^6 beta cells present in the 4,000 human islets previously found to be required for the long-term reversal of diabetes. Hence, the observed reduction in BG levels, but lack of complete diabetes reversal in mice bearing hESC-derived transplants, is not unexpected given this technical constraint. Taken together, our *in vivo* data demonstrate that hESC-derived beta-like cells maintain their differentiated phenotype and remain glucose responsive after a short engraftment period *in vivo* and highlight their potential therapeutic value.

Discussion

Herein, we describe a simplified differentiation protocol replicating key steps of embryonic pancreas organogenesis for the defined generation of human pancreatic progenitor and endocrine cell types from hESCs that results in the formation of glucose-responsive beta-like cells *in vitro*. hESC-derived beta-like cells exhibit key features of cadaveric human beta cells both *in vitro* and *in vivo*, most notably their ability to respond to physiological increases in glucose concentrations by secreting insulin. Gene expression analysis of beta-like cells indicates the presence of factors essential for beta cell function, proper biosynthesis of mature insulin, glucose metabolism, and insulin secretion at levels comparable to human islets. In addition, beta-like cells display ultrastructural features of *bona fide* human beta cells, such as appropriate secretory vesicles. Thus, critical elements necessary for the generation and appropriate processing, packaging, and storing of insulin in its bioactive mature form are present in these hESC-derived cells. Finally, beta-like cells remained functional after short-term transplantation and reduced blood glucose levels in a murine model of diabetes, further confirming the correct differentiation state of the cells.

Recently, two other groups have reported the derivation of glucose-responsive beta-like cells from hESCs that share many characteristics of the beta-like cells described here (Pagliuca *et al*, 2014; Rezania *et al*, 2014). However, both studies focused on optimizing the later stages of direct differentiation, while employing parts of published protocols, namely the addition of RCN, to establish pancreatic progenitor populations. Our data demonstrate that the generation of pancreatic progenitors using this method also results in the undesirable generation of immature polyhormonal endocrine cells that lack expression of the critical beta cell transcription factor NKX6.1. Indeed, both published studies do note appreciable populations of C-peptide/insulin-positive cells that lack NKX6.1 expression. We demonstrate that polyhormonal cells result from precocious endocrine induction in $PDX1^+$ pancreatic progenitors (lacking NKX6.1 expression), which can be avoided by omitting BMP inhibitors during the pancreas specification stage. Further, our detailed analysis of the effects of individual RCN factors on the expression of key pancreatic markers revealed that retinoic acid alone is sufficient to induce proficient generation of more than 98% $PDX1^+$ pancreatic progenitors. Subsequent exposure to EGF and KGF results in the rapid and effective activation of NKX6.1 in these cells, generating $PDX1^+/NKX6.1^+$ progenitor cells with the ability to

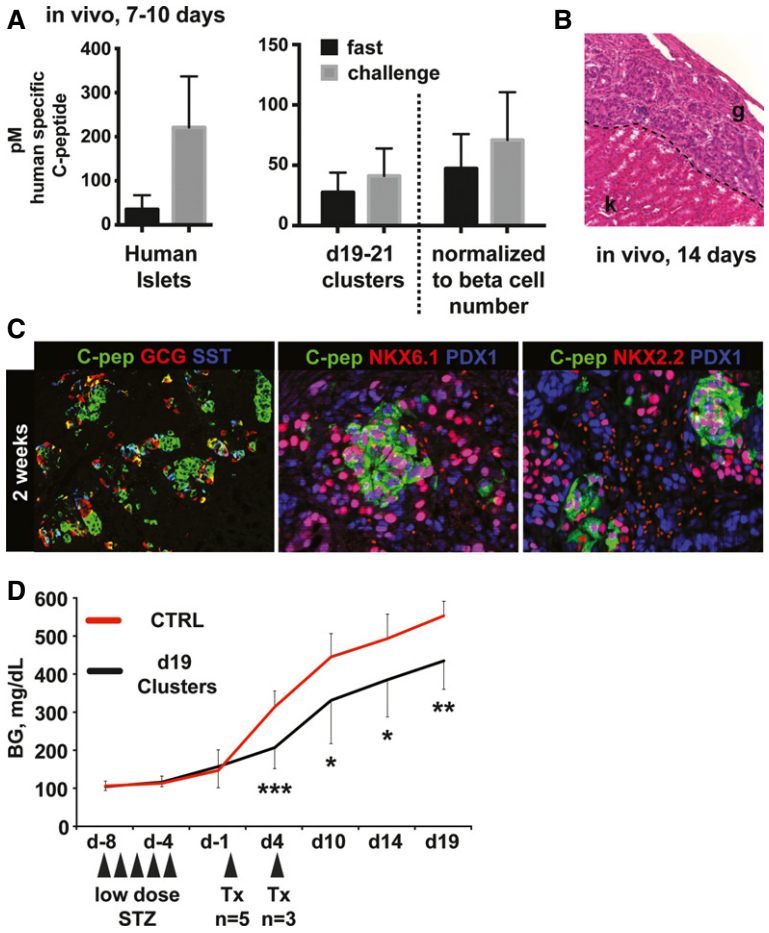

Figure 6. Beta-like cells remain glucose responsive after short-term transplantation.

A Levels of circulating human C-peptide measured in sera of mice 7–10 days after transplantation with either 4,000 human islets or 5.0×10^6 direct differentiated cells (containing approximately 1.15×10^6 beta-like cells). Fasting and challenge sera were collected following an overnight fast and 1 h after intraperitoneal glucose challenge, respectively. Dashed line separates raw data from serum C-peptide measurements normalized to the number of beta cells present in each human islet graft (4,000 human islets transplanted each containing ~1,000 cells, approximately 50% of which are beta cells, hence 2.0×10^6 beta cells present in grafts total). $n = 5$ for human islets and $n = 12$ for hESC-derived grafts.

B Hematoxylin and eosin staining of day 14 graft. k, kidney; g, graft. Representative data from one of three mice are shown.

C Immunofluorescence staining of differentiated hESC grafts 2 weeks post-transplantation for human C-peptide, glucagon (GCG), somatostatin (SST), PDX1, NKX6.1, and NKX2.2. Representative data from one of three mice are shown.

D Blood glucose (BG) levels of mice treated with streptozotocin to ablate endogenous beta cells (STZ) followed by transplantation (Tx) of beta-like cell containing clusters either at day 0 or at day 4 as indicated ($n = 8$, two independent differentiation experiments). Values are average ± SD. Statistical significance was calculated using two-tailed t-test. $^*P < 0.05$, $^{**}P < 0.01$, and $^{***}P < 0.001$. Control (CTRL) group: 6–9 animals.

give rise to beta-like cells *in vitro*. These simplified differentiation conditions enable the efficient generation of human pancreatic and more restricted endocrine progenitor populations from pluripotent stem cells without unwanted formation of polyhormonal cells. Thus, we conclude that this simplified differentiation protocol more closely resembles key aspects of early human pancreas development and, as such, represents an improvement over published protocols.

Although the mechanisms of endocrine differentiation *in vivo* are not completely understood, previous studies in rodents have shown an important role for Notch signaling. While initially required for the generation of competent progenitor cells, a subsequent reduction of Notch signaling is necessary for the induction of Neurog3 expression that initiates endocrine differentiation (Shih *et al*, 2012). In the context of *in vitro* differentiation, previous studies have shown that direct inhibition of Notch signaling by gamma secretase inhibitors or the use of BMP and TGFβ/ALK inhibitors results in increased insulin expression at later stages (Mfopou *et al*, 2010; Nostro *et al*, 2011; Pagliuca *et al*, 2014; Rezania *et al*, 2014). We employed BMP and ALK inhibition over a 5-day window to induce NEUROG3 expression specifically in $PDX1^+/NKX6.1^+$ progenitors, which resulted in the efficient generation of $INS^+/NKX6.1^+$ beta-like cells, while only few polyhormonal cells were observed (~3%). Likely these unwanted cells originate from the small percentage of PDX1 pancreatic progenitors present at the time of endocrine induction. In contrast to the formation of $PDX1^+$ and $PDX1^+/NKX6.1^+$ progenitors that occurs rapidly (36–48 h after the addition of inducing factor(s) and uniformly in the majority of cells, endocrine differentiation occurs over a prolonged period and is confined to a small

subset of total cells. This might be a reflection of the situation observed during normal human pancreas development where only few progenitor cells initiate the endocrine differentiation program at any given time (Jennings *et al*, 2013). While simultaneous widespread induction of endocrine differentiation in a majority of $PDX1^+/NKX6.1^+$ progenitor population would greatly reduce differentiation time and increase beta-like cell yield, our results point to a regulation of NEUROG3 expression that requires subtle, yet temporally precise adjustment that appears more complex than just Notch inhibition. As our differentiation protocol allows for a tight control of NEUROG3 expression, it could be used in future studies to identify novel regulators of NEUROG3 gene expression, and ideally to achieve uniform NEUROG3 activation during direct differentiation *in vitro*.

While cadaveric islet preparations are widely accepted as the gold standard for studying human beta cells, several problems associated with their use remain. For example, their performance and utility depend on a number of confounding factors: genetic variance, age and life style of the donor, isolation time, islet purity, and shipping conditions. By eliminating the constraints of availability and reproducibility, we anticipate that hESC-derived beta-like cells will provide an important tool in accelerating a more complete understanding of the biology of human beta cells.

Taken together, our fast and simplified protocol provides precise temporal control over the generation of subsequent pancreatic progenitor and endocrine cell types and results in the establishment of human beta-like cells that exhibit glucose responsiveness *in vitro* and *in vivo*. Our suspension-based direct differentiation approach is scalable, and our ability to produce large numbers of beta-like cells will further accelerate efforts in delivering a safe and efficient cell therapy to patients suffering from diabetes. Furthermore, through the production and maintenance of different developmental cell populations, our approach can be used for more detailed investigations into human pancreas development and human beta cell function that were previously impossible due to limited donor material, such as large-scale drug screens and genomewide gene function studies.

Material and Methods

Cell culture

Undifferentiated MEL1 $INS^{GFP/W}$ reporter cells (Micallef *et al*, 2012) were maintained on mouse embryo fibroblast feeder layers (Millipore) in hESC media as described (Guo *et al*, 2013b). Suspension-based differentiations were carried out as follows. Briefly, confluent cultures were dissociated into single-cell suspension by incubation with TrypLE (Gibco). Cells were counted and each well of 6-well low-adherence plates were seeded with 5.5×10^6 cells in 5.5 ml hESC media supplemented with 10 ng/ml activin A (R&D Systems) and 10 ng/ml heregulin-b1 (Peprotech). Plates were placed on an orbital shaker at 100 rpm to induce sphere formation as described (Schulz *et al*, 2012). To induce definitive endoderm differentiation, aggregates were collected 24 h later in a 50-ml falcon tube, allowed to settle by gravity, washed once with PBS, and re-suspended in d1 media [RPMI (Gibco) containing 0.2% FBS, 1:5,000 ITS (Gibco), 100 ng/ml activin A, and 50 ng/ml WNT3a (R&D Systems)]. Clusters from three wells were combined into two wells at this point and distributed into fresh low attachment plates in 5.5 ml d1 media. Media thereafter were changed daily, by removing either 4.5 ml media (at the end of d1) or 5.5 ml media the following days and adding back 5.5 ml fresh media until day 9. After day 9, only 5 ml of media was removed and added daily. Differentiation employing published protocols has been described (Rezania *et al*, 2012; Schulz *et al*, 2012). Media in our simplified differentiation protocol consist of the following: d2: RPMI containing 0.2% FBS, 1:2,000 ITS, and 100 ng/ml activin A; d3: RPMI containing 0.2% FBS, 1:1,000 ITS, 2.5 μM TGFbi IV (CalBioChem), and 25 ng/ml KGF (R&D Systems); d4-5: RPMI containing 0.4% FBS, 1:1,000 ITS, and 25 ng/ml KGF; d6-7: DMEM (Gibco) with 25 mM glucose containing 1:100 B27 (Gibco), 3 nM TTNBP (Sigma); d8: DMEM with 25 mM glucose containing 1:100 B27, 3 nM TTNBP, and 50 ng/ml EGF (R&D Systems); d9: DMEM with 25 mM glucose containing 1:100 B27, 50 ng/ml EGF, and 50 ng/ml KGF; d10-14: DMEM with 25 mM glucose containing 1:100 B27, 500 nM LDN-193189 (Stemgent), 30 nM TBP (Millipore), 1,000 nM ALKi II (Axxora), and 25 ng/ml KGF; and d15-21: DMEM with 2.8 mM glucose containing 1:100 Glutamax (Gibco) and 1:100 NEAA (Gibco). Human islets were from Prodo Laboratories or the UCSF Islets and Cellular Production Facility.

Mice

NOD.Cg-*Prkdcscid Il2rgtm1Wjl*/SzJ mice (NSG) were obtained from Jackson Laboratories. Mice used in this study were maintained according to protocols approved by the University of California, San Francisco Committee on Laboratory Animal Resource Center. For kidney capsule grafts, approximately 5.0×10^6 hESC-differentiated cells in spheres and 4,000 human islet equivalents were transplanted as described (Szot *et al*, 2007; Russ & Efrat, 2011). For glucose-induced insulin secretion, mice were fasted overnight and serum was collected before and after intraperitoneal administration of 3 g/kg D-glucose solution. For induction of diabetes, mice were administered 35 mg/kg streptozotocin via intraperitoneal injection for 5 days. Graft-bearing kidneys were removed for immunofluorescence analysis. No statistical method was employed to determine sample size, mice were not randomized, and analysis was not blinded.

Cell sorting and flow cytometric analysis

Briefly, spheres were collected and allowed to settle by gravity. Clusters were washed once in PBS and dissociated by gentle pipetting after 12- to 15-min incubation in Accumax (innovative cell technologies). For sorting, cell suspension were filtered and re-suspended in FACS buffer consisting of PBS (UCSF cell culture facility) containing 2 mM EDTA (Ambion) and 1% BSA (Sigma). Dead cells were excluded by DAPI (Sigma) staining. Cell sorting was performed on a FACSAria II (BD Bioscience). For flow-based analysis, dissociated cells were fixed with 4% paraformaldehyde (Electron Microscopy Science) for 15 min at room temperature, followed by two washes in PBS. Samples were either stored at 4°C or immediately stained with directly conjugated antibodies. Data analysis was performed with FlowJo software. Mouse glucagon and mouse human C-peptide antibodies were conjugated in-house by the UCSF Antibody Core and/or with Antibody Labeling Kits (Molecular Probes) according to manufacturer's instructions. Commercially available directly conjugated antibodies are listed below:

Antibody	Manufacturer
Human PAX6–Alexa647	BD Bioscience
Islet-1–PE	BD Bioscience
NKX6.1–Alexa647	BD Bioscience
NKX6.1-PE	BD Bioscience
Chromogranin A–PE	BD Bioscience
NeuroD1–Alexa647	BD Bioscience
PDX1-PE	BD Bioscience
Ki-67–Alexa647	BD Bioscience

Electron microscopic analysis

Spheres were fixed by adding 37°C warm 0.1 M sodium cacodylate solution (Sigma) containing 2% paraformaldehyde (Electron Microscopy Science) and 2.5% glutaraldehyde (Electron Microscopy Science), 3 μM $CaCl_2$ (Sigma), final pH 7.4. Spheres were then transferred to 4°C for approximately 18 h, followed by standard processing and analysis by the Electron Microscope Lab/Diabetes Center Microscope Core.

Immunofluorescence analysis

Spheres were fixed for 15–30 min at room temperature with 4% paraformaldehyde, followed by multiple washes in PBS. Whole-mount staining was performed in suspension, by first blocking overnight at 4°C in blocking buffer consisting of CAS-block (Invitrogen) with 0.2% Triton X-100 (Fisher). Primary antibodies were incubated overnight at 4°C in blocking buffer, followed by washes in PBS containing 0.1% Tween-20 (PBS-T, Sigma) and incubation in appropriate secondary antibodies diluted in PBS-T overnight at 4°C. The next day, clusters were washed in PBS-T followed by PBS and mounted with Vectashield (Vector) on glass slides. For sectioning of clusters, spheres were embedded in 2% agar (Sigma), followed by dehydration, paraffin embedding, and sectioning. Cut sections were rehydrated and treated with and antigen retrieval solution (Biogenex) before incubation in primary antibodies overnight at 4°C in blocking buffer. The next day, sections were washed three times in PBS-T and incubated with appropriate secondary antibodies for 30–40 min at room temperature in PBS-T. Appropriate Alexa-conjugated secondary antibodies were purchased from JAX or Molecular Probes and used at 1:500 dilutions. Slides were washed in PBS-T and PBS before mounting in Vectashield. Nuclei were visualized with DAPI. Images were acquired using a Leica SP5 microscope or a Zeiss ApoTome. Primary antibodies were employed as follows:

Antigen	Species	Dilution	Manufacturer
Human C-peptide	Mouse	1:200	Chemicon
Human C-peptide	Rat	1:1,000	DSHB
Insulin	Mouse	1:1,000	Sigma
Insulin	Guinea pig	1:500	DAKO
Glucagon	Mouse	1:1,000	Sigma
NKX6.1	Mouse	1:100	DSHB
NKX2.2	Mouse	1:20	DSHB
PDX1	Goat	1:200	R&D Systems
Human NEUROG3	Sheep	1:300	R&D Systems
Ki-67	Rabbit	1:100	NovoCastra

qPCR analysis

Total RNA was isolated with TRIzol (Sigma) or micro/mini RNeasy kit (Qiagen) and reverse-transcribed using the iScript cDNA Kit (Bio-Rad) according to manufacturer's instructions. qPCR analysis was performed on an ABI 7900 HT Fast Real-Time PCR System (Applied Biosystems) and CFX Connect Real-Time System (Bio-Rad) using standard protocols. Primers were TaqMan probes (Applied Biosystems) and/or as published previously (Liu *et al*, 2014). *P*-values were calculated using a two-tailed Student's *t*-test.

Content analysis

Insulin, human C-peptide, and proinsulin analyses were performed by measuring an aliquot of acidic ethanol lysed clusters with commercially available ELISA kits (insulin cat. 80-INSMR-CH10, human C-peptide cat. 80-CPTHU-CH01, and proinsulin cat. 80-PINHUT-CH01; all from Alpco). Total DNA was quantified by PicoGreen (Invitrogen) assay and normalized to the percentage of C-peptide-positive cells in each sample.

Western blotting for proinsulin/insulin

Cell lysates were resolved on 4–12% acrylamide gradient SDS–PAGE gels (NuPAGE, Invitrogen) normalized to cellular DNA (Quant-iT dsDNA, Molecular Probes). The samples were then electrotransferred to nitrocellulose membranes and immunoblotted with guinea pig anti-insulin, which recognizes both proinsulin and insulin, as previously described (Haataja *et al*, 2013). Immunoblotting with anti-tubulin was used as a confirmatory loading control. HRP-conjugated secondary antibodies (Jackson ImmunoResearch) were used for enhanced chemiluminescence detection (Millipore). The analysis was performed four times with isolated human islets used as a positive control.

Glucose-stimulated insulin secretion

Human islets or hESC-derived spheres were transferred into tubes and washed twice with Krebs–Ringer Bicarbonate buffer (KRB) containing 2.8 mM glucose. Samples were incubated for one hour in 2.8 mM glucose containing KRB to allow equilibration of cells. 2.8 mM buffer was removed and replaced with fresh KRB containing 2.8 mM glucose for one hour followed by incubation for another hour in KRB containing 16.7 mM glucose. After the incubation period, buffers were collected for human C-peptide-specific ELISA analysis using a commercially available kit (Alpco).

Supplementary information for this article is available online: http://emboj.embopress.org

Acknowledgements†

We thank members of the Hebrok laboratory and UCSF Diabetes Center for helpful comments and discussion. HAR was supported by a Richard G. Klein Fellowship and JDRF Fellowship (3-2012-266); TGH was supported by NIDDK training grant #T32DK007418. Imaging and flow cytometry experiments were supported by resources from the UCSF Diabetes and Endocrinology Research Center (DERC) and UCSF Flow Cytometry Core. Image acquisition was supported by the University of California, San Francisco Diabetes and Endocrinology Research Center (DERC) microscopy core P30 DK63720. We would like to thank Larry Ackerman for expert help with electron microscopy. Research in the laboratory of PA was supported by NIH R01 DK48280. Work in the lab of VC was supported by the Life Sciences Discovery Fund grant #4553677 and JDRF grant #17-2011-620. Stem cell research in the laboratory of MH is supported by a grant from the Leona M. and Harry B. Helmsley Charitable Trust (2012PG-T1D017). MH and PA acknowledge assistance from the Brehm Coalition for Discovery in Diabetes.

Author contributions

HAR, AVP, and MH designed, analyzed, and interpreted results. SP, VC, RB, GLS, and PA interpreted results. HAR, AVP, JJR, MS, TGH, LH, GLS, and TG performed experiments. HAR, AVP, TGH, and MH wrote the manuscript. HAR, AVP, JJR, TGH, GGN, and MH contributed to manuscript revision. All authors reviewed, edited, and approved the manuscript.

Conflict of interest

The authors declare that they have no conflict of interest.

References

Barton FB, Rickels MR, Alejandro R, Hering BJ, Wease S, Naziruddin B, Oberholzer J, Odorico JS, Garfinkel MR, Levy M, Pattou F, Berney T, Secchi A, Messinger S, Senior PA, Maffi P, Posselt A, Stock PG, Kaufman DB, Luo X *et al* (2012) Improvement in outcomes of clinical islet transplantation: 1999–2010. *Diabetes Care* 35: 1436 – 1445

Bouwens L, Houbracken I, Mfopou JK (2013) The use of stem cells for pancreatic regeneration in diabetes mellitus. *Nat Rev Endocrinol* 9: 598 – 606

Cabrera O, Berman DM, Kenyon NS, Ricordi C, Berggren P-O, Caicedo A (2006) The unique cytoarchitecture of human pancreatic islets has implications for islet cell function. *Proc Natl Acad Sci USA* 103: 2334 – 2339

Chen S, Borowiak M, Fox JL, Maehr R, Osafune K, Davidow L, Lam K, Peng LF, Schreiber SL, Rubin LL, Melton D (2009) A small molecule that directs differentiation of human ESCs into the pancreatic lineage. *Nat Chem Biol* 5: 258 – 265

D'Amour KA, Agulnick AD, Eliazer S, Kelly OG, Kroon E, Baetge EE (2005) Efficient differentiation of human embryonic stem cells to definitive endoderm. *Nat Biotechnol* 23: 1534 – 1541

D'Amour KA, Bang AG, Eliazer S, Kelly OG, Agulnick AD, Smart NG, Moorman MA, Kroon E, Carpenter MK, Baetge EE (2006) Production of pancreatic hormone-expressing endocrine cells from human embryonic stem cells. *Nat Biotechnol* 24: 1392 – 1401

De Krijger RR, Aanstoot HJ, Kranenburg G, Reinhard M, Visser WJ, Bruining GJ (1992) The midgestational human fetal pancreas contains cells coexpressing islet hormones. *Dev Biol* 153: 368 – 375

Efrat S, Russ HA (2012) Making β cells from adult tissues. *Trends Endocrinol Metab* 23: 278 – 285

Fiaschi-Taesch NM, Salim F, Kleinberger J, Troxell R, Cozar-Castellano I, Selk K, Cherok E, Takane KK, Scott DK, Stewart AF (2010) Induction of human -cell proliferation and engraftment using a single G1/S regulatory molecule, cdk6. *Diabetes* 59: 1926 – 1936

Gu G, Dubauskaite J, Melton DA (2002) Direct evidence for the pancreatic lineage: NGN3+ cells are islet progenitors and are distinct from duct progenitors. *Development* 129: 2447 – 2457

Guo S, Dai C, Guo M, Taylor B, Harmon JS, Sander M, Robertson RP, Powers AC, Stein R (2013a) Inactivation of specific β cell transcription factors in type 2 diabetes. *J Clin Invest* 123: 3305 – 3316

Guo T, Landsman L, Li N, Hebrok M (2013b) Factors expressed by murine embryonic pancreatic mesenchyme enhance generation of insulin-producing cells from hESCs. *Diabetes* 62: 1581 – 1592

Haataja L, Snapp E, Wright J, Liu M, Hardy AB, Wheeler MB, Markwardt ML, Rizzo M, Arvan P (2013) Proinsulin intermolecular interactions during secretory trafficking in pancreatic β cells. *J Biol Chem* 288: 1896 – 1906

Hebrok M (2003) Hedgehog signaling in pancreas development. *Mech Dev* 120: 45 – 57

Hebrok M (2012) Generating β cells from stem cells-the story so far. *Cold Spring Harb Perspect Med* 2: a007674

Herrera PL, Népote V, Delacour A (2002) Pancreatic cell lineage analyses in mice. *Endocrine* 19: 267 – 278

Hua H, Shang L, Martinez H, Freeby M, Gallagher MP, Ludwig T, Deng L, Greenberg E, Leduc C, Chung WK, Goland R, Leibel RL, Egli D (2013) iPSC-derived β cells model diabetes due to glucokinase deficiency. *J Clin Invest* 123: 3146 – 3153

Jennings RE, Berry AA, Kirkwood-Wilson R, Roberts NA, Hearn T, Salisbury RJ, Blaylock J, Piper Hanley K, Hanley NA (2013) Development of the human pancreas from foregut to endocrine commitment. *Diabetes* 62: 3514 – 3522

Johansson KA, Dursun U, Jordan N, Gu G, Beermann F, Gradwohl G, Grapin-Botton A (2007) Temporal control of neurogenin3 activity in pancreas progenitors reveals competence windows for the generation of different endocrine cell types. *Dev Cell* 12: 457 – 465

Kelly OG, Chan MY, Martinson LA, Kadoya K, Ostertag TM, Ross KG, Richardson M, Carpenter MK, D'Amour KA, Kroon E, Moorman M, Baetge EE, Bang AG (2011) Cell-surface markers for the isolation of pancreatic cell types derived from human embryonic stem cells. *Nat Biotechnol* 29: 750 – 756

Kroon E, Martinson LA, Kadoya K, Bang AG, Kelly OG, Eliazer S, Young H, Richardson M, Smart NG, Cunningham J, Agulnick AD, D'Amour KA, Carpenter MK, Baetge EE (2008) Pancreatic endoderm derived from human embryonic stem cells generates glucose-responsive insulin-secreting cells in vivo. *Nat Biotechnol* 26: 443 – 452

Liu H, Yang H, Zhu D, Sui X, Li J, Liang Z, Xu L, Chen Z, Yao A, Zhang L, Zhang X, Yi X, Liu M, Xu S, Zhang W, Lin H, Xie L, Lou J, Zhang Y, Xi J *et al* (2014) Systematically labeling developmental stage-specific genes for the study of pancreatic. *Cell Res* 24: 1181 – 1200

Maehr R, Chen S, Snitow M, Ludwig T, Yagasaki L, Goland R, Leibel RL, Melton DA (2009) Generation of pluripotent stem cells from patients with type 1 diabetes. *Proc Natl Acad Sci USA* 106: 15768 – 15773

Mfopou JK, Chen B, Mateizel I, Sermon K, Bouwens L (2010) Noggin, retinoids, and fibroblast growth factor regulate hepatic or pancreatic fate of human embryonic stem cells. *Gastroenterology* 138: 2233 – 2245, 2245.e14

†Correction added on 2 July 2015 after first online publication: The Acknowledgements section has been corrected by removing incorrect funding information.

Micallef SJ, Li X, Schiesser JV, Hirst CE, Yu QC, Lim SM, Nostro MC, Elliott DA, Sarangi F, Harrison LC, Keller G, Elefanty AG, Stanley EG (2012) INS(GFP/w) human embryonic stem cells facilitate isolation of in vitro derived insulin-producing cells. *Diabetologia* 55: 694 – 706

Murtaugh LC, Melton DA (2003) Genes, signals, and lineages in pancreas development. *Annu Rev Cell Dev Biol* 19: 71 – 89

Nostro MC, Sarangi F, Ogawa S, Holtzinger A, Corneo B, Li X, Micallef SJ, Park I-H, Basford C, Wheeler MB, Daley GQ, Elefanty AG, Stanley EG, Keller G (2011) Stage-specific signaling through TGFβ family members and WNT regulates patterning and pancreatic specification of human pluripotent stem cells. *Development* 138: 861 – 871

Nostro M-C, Keller G (2012) Generation of beta cells from human pluripotent stem cells: potential for regenerative medicine. *Semin Cell Dev Biol* 23: 701 – 710

Pagliuca FW, Melton DA (2013) How to make a functional β-cell. *Development* 140: 2472 – 2483

Pagliuca FW, Millman JR, Gürtler M, Segel M, Van Dervort A, Ryu JH, Peterson QP, Greiner D, Melton DA (2014) Generation of functional human pancreatic b cells in vitro. *Cell* 159: 428 – 439

Pan FC, Wright C (2011) Pancreas organogenesis: from bud to plexus to gland. *Dev Dyn* 240: 530 – 565

Posselt AM, Szot GL, Frassetto LA, Masharani U, Tavakol M, Amin R, McElroy J, Ramos MD, Kerlan RK, Fong L, Vincenti F, Bluestone JA, Stock PG (2010) Islet transplantation in type 1 diabetic patients using calcineurin inhibitor-free immunosuppressive protocols based on T-Cell adhesion or costimulation blockade. *Transplantation* 90: 1595 – 1601

Rezania A, Riedel MJ, Wideman RD, Karanu F, Ao Z, Warnock GL, Kieffer TJ (2011) Production of functional glucagon-secreting α-cells from human embryonic stem cells. *Diabetes* 60: 239 – 247

Rezania A, Bruin JE, Riedel MJ, Mojibian M, Asadi A, Xu J, Gauvin R, Narayan K, Karanu F, O'Neil JJ, Ao Z, Warnock GL, Kieffer TJ (2012) Maturation of human embryonic stem cell-derived pancreatic progenitors into functional islets capable of treating pre-existing diabetes in mice. *Diabetes* 61: 2016 – 2029

Rezania A, Bruin JE, Arora P, Rubin A, Batushansky I, Asadi A, O'Dwyer S, Quiskamp N, Mojibian M, Albrecht T, Yang YHC, Johnson JD, Kieffer TJ (2014) Reversal of diabetes with insulin-producing cells derived in vitro from human pluripotent stem cells. *Nat Biotechnol* 32: 1121 – 1133

Riedel MJ, Asadi A, Wang R, Ao Z, Warnock GL, Kieffer TJ (2011) Immunohistochemical characterisation of cells co-producing insulin and glucagon in the developing human pancreas. *Diabetologia* 55: 372 – 381

Roark R, Itzhaki L, Philpott A (2012) Complex regulation controls Neurogenin3 proteolysis. *Biol Open* 1: 1264 – 1272

Russ HA, Efrat S (2011) In-vivo functional assessment of engineered human insulin-producing cells. In *Cell Transplantation*, Soto-Gutierrez A, Navarro-Alvarez N, Fox IJ (eds.), Methods in Bioengineering, Yarmush ML, Langer RS (eds.), pp. 35 – 46. Norwood, MA: Artech House

Schaffer AE, Freude KK, Nelson SB, Sander M (2010) Nkx6 transcription factors and Ptf1a function as antagonistic lineage determinants in multipotent pancreatic progenitors. *Dev Cell* 18: 1022 – 1029

Schulz TC, Young HY, Agulnick AD, Babin MJ, Baetge EE, Bang AG, Bhoumik A, Cepa I, Cesario RM, Haakmeester C, Kadoya K, Kelly JR, Kerr J, Martinson LA, McLean AB, Moorman MA, Payne JK, Richardson M, Ross KG, Sherrer ES *et al* (2012) A scalable system for production of functional pancreatic progenitors from human embryonic stem cells. *PLoS ONE* 7: e37004

Seymour PA, Sander M (2011) Historical perspective: beginnings of the -cell: current perspectives in -cell development. *Diabetes* 60: 364 – 376

Shang L, Hua H, Foo K, Martinez H, Watanabe K, Zimmer M, Kahler DJ, Freeby M, Chung W, Leduc C, Goland R, Leibel RL, Egli D (2014) β-cell dysfunction due to increased ER stress in a stem cell model of Wolfram syndrome. *Diabetes* 63: 923 – 933

Shapiro AM, Lakey JR, Ryan EA, Korbutt GS, Toth E, Warnock GL, Kneteman NM, Rajotte RV (2000) Islet transplantation in seven patients with type 1 diabetes mellitus using a glucocorticoid-free immunosuppressive regimen. *N Engl J Med* 343: 230 – 238

Shih HP, Kopp JL, Sandhu M, Dubois CL, Seymour PA, Grapin-Botton A, Sander M (2012) A Notch-dependent molecular circuitry initiates pancreatic endocrine and ductal cell differentiation. *Development* 139: 2488 – 2499

Shim JH, Kim J, Han J, An SY, Jang YJ, Son J, Woo DH, Kim SK, Kim JH (2014) Pancreatic islet-like three dimensional aggregates derived from human embryonic stem cells ameliorate hyperglycemia in streptozotocin-induced diabetic mice. *Cell Transplant* doi: 10.3727/096368914X685438

Szot GL, Koudria P, Bluestone JA (2007) Transplantation of pancreatic islets into the kidney capsule of diabetic mice. *J Vis Exp* e404, doi: 10.3791/404

Szot GL, Yadav M, Lang J, Kroon E, Kerr J, Kadoya K, Brandon EP, Baetge EE, Bour-Jordan H, Bluestone JA (2015) Tolerance induction and reversal of diabetes in mice transplanted with human embryonic-stem-cell-derived pancreatic endoderm. *Cell Stem Cell* 16: 148 – 157

Tudurí E, Kieffer TJ (2011) Reprogramming gut and pancreas endocrine cells to treat diabetes. *Diabetes Obes Metab* 13(Suppl 1): 53 – 59

Van Hoof D, Mendelsohn AD, Seerke R, Desai TA, German MS (2011) Differentiation of human embryonic stem cells into pancreatic endoderm in patterned size-controlled clusters. *Stem Cell Res* 6: 276 – 285

Xu X, Browning V, Odorico JS (2011) Activin, BMP and FGF pathways cooperate to promote endoderm and pancreatic lineage cell differentiation from human embryonic stem cells. *Mech Dev* 128: 412 – 427

Zhou Q, Melton DA (2008) Extreme makeover: converting one cell into another. *Cell Stem Cell* 3: 382 – 388

